

Competition between Two-Photon Driving, Dissipation, and Interactions in Bosonic Lattice Models: An Exact Solution

David Roberts^{1,2,*} and A. A. Clerk¹¹*Pritzker School of Molecular Engineering, University of Chicago, Chicago, 60637 Illinois, USA*²*Department of Physics, University of Chicago, Chicago, 60637 Illinois, USA*
 (Received 22 August 2022; accepted 6 January 2023; published 6 February 2023)

We present an exact solution in arbitrary dimensions for the steady states of a class of quantum driven-dissipative bosonic models, where a set of modes is subject to arbitrary two-photon driving, single-photon loss, and a global Hubbard (or Kerr)-like interaction. Our solutions reveal a wealth of striking phenomena, including the emergence of dissipative phase transitions, nontrivial mode competition physics and symmetry breaking, and the stabilization of many-body SU(1,1) pair-coherent states. Our exact solutions enable the description of spatial correlations, and are fully valid in regimes where traditional mean-field and semiclassical approaches break down.

DOI: [10.1103/PhysRevLett.130.063601](https://doi.org/10.1103/PhysRevLett.130.063601)

Introduction.—Spurred both by applications to quantum information and the advent of controllable dissipative quantum simulators [1–5] there is a renewed interest in exploring driven-dissipative bosonic quantum systems in the many-body limit (see, e.g., Refs. [6–15]). Of particular interest are the possibility of dissipative quantum phase transitions, and the emergence of highly nonthermal steady states. While a variety of numerical approaches have been devised to study such systems, they have limitations. Conventional Gutzwiller mean-field approaches (see, e.g., Refs. [16–19]) are unable to account for strong correlations, whereas matrix-product state methods (see, e.g., Ref. [20]) are largely restricted to 1D systems. Alternate numerical approaches for 2D exist [21,22], but these can become numerically infeasible for large systems. Given this, the ability to have exact analytic solutions for higher dimensional models would be extremely valuable.

In this Letter, we address this outstanding challenge. We introduce a class of strongly interacting driven-dissipative bosonic models, and show that it is possible to *analytically* describe their dissipative steady states in arbitrary dimensions. The basic system is shown in Fig. 1: a set of bosonic modes is subject to arbitrary two-photon driving (both on site, and between sites), as well as to Markovian single-photon loss and a global Hubbard (Kerr) interaction that depends on total photon number. While there are no conventional hopping interactions, one still has a lattice structure defined by the intersite two-photon drives. We

show that the steady-state density matrix of this model is amenable to exact solution via the hidden time-reversal symmetry (HTRS) method [23,24]. This method is related to other quantum optical solution methods [25–29], though attempts to use these in the many-body limit were unsuccessful [30,31].

Our exact solution reveals a wealth of physical phenomena. For weak driving, one sees the emergence of phase transition behavior as system size is increased, with singularities arising in the thermodynamic limit from the merging of discrete photonic resonances. Unlike well-studied single-site models [32], the phase transition physics here can occur far from the many-photon semiclassical limit, and can show marked deviations from mean-field

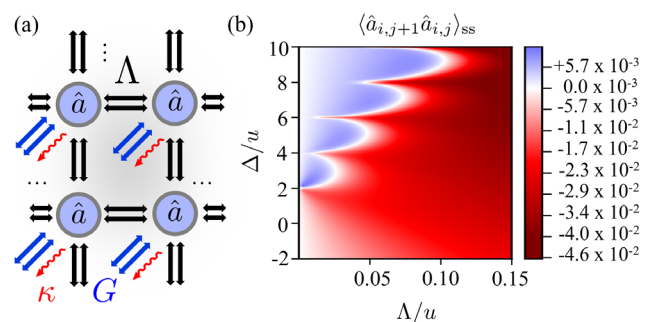


FIG. 1. (a) Schematic of the model: a lattice of bosonic modes, with two-photon drives on each site (G) and on each nearest-neighbor (nn) bond (Λ). There is also single-photon loss κ on each site, and a global Hubbard (Kerr) interaction U . (b) Our exact solution allows the description of steady-state spatial correlations. Here, nn pairing correlations are plotted as a function of drive detuning Δ and drive amplitude Λ , for a $N = 225$ site 2D lattice with $u \equiv U/N$, $\kappa = 0.01u$. One sees clearly a Mott-lobe-like structure associated with multiphoton resonances.

Published by the American Physical Society under the terms of the [Creative Commons Attribution 4.0 International license](https://creativecommons.org/licenses/by/4.0/). Further distribution of this work must maintain attribution to the author(s) and the published article's title, journal citation, and DOI.

theory predictions. We also show surprising connections to the representation theory of $SU(1,1)$. Strikingly, we find that with appropriate tuning, the driven-dissipative steady state is directly related to a nontrivial many-body generalization of $SU(1,1)$ pair-coherent states [33–35].

We also find surprising behavior in more strongly driven regimes: the system can exhibit surprising symmetry breaking phenomena and mode-competition physics, with the exact solution again providing crucial insights. We stress that the class of models we study could be directly realized in, e.g., superconducting quantum circuit experiments, and can be viewed as a many-body extension of the driven Kerr parametric oscillator systems that are being studied extensively in the context of bosonic error correction [36,37].

Two-photon driven global interaction models.—We consider a set of N bosonic modes (lowering operators \hat{a}_j), subject to arbitrary two-photon (parametric) drives (amplitudes M_{ij}), as well as a global Hubbard interaction (i.e., equal-magnitude self-Kerr and cross-Kerr interactions U/N). Assuming all drives to have an identical detuning Δ from resonance, and working in the common rotating frame, the coherent system dynamics is given by

$$\hat{H} = \frac{U}{N} \left(\sum_j \hat{n}_j \right)^2 - \Delta \sum_j \hat{n}_j + \sum_{i,j} (M_{ij} \hat{a}_i^\dagger \hat{a}_j^\dagger + \text{H.c.}) \quad (1)$$

where $\hat{n}_j \equiv \hat{a}_j^\dagger \hat{a}_j$. While our solution technique is more general, we focus here on the case where our modes live on the sites of a D -dimensional hypercubic lattice, and we have translational invariance, with $M_{ii} = G$, and off diagonals $M_{ij} = \Lambda/2D$ if i, j are nearest-neighbor sites, and zero otherwise. This represents a modified two-photon driven Bose-Hubbard model, with single-particle hopping replaced with p -wave pairing terms, and the interaction made global. We also include dissipation: independent Markovian single-particle loss on each site. The full dynamics is thus described by the Lindblad master equation

$$\partial_t \hat{\rho} = -i[\hat{H}, \hat{\rho}] + \sum_j \kappa \mathcal{D}[\hat{a}_j] \hat{\rho} \equiv \mathcal{L} \hat{\rho}, \quad (2)$$

where $\mathcal{D}[\hat{X}] \hat{\rho} \equiv \hat{X} \hat{\rho} \hat{X}^\dagger - (1/2) \{ \hat{X}^\dagger \hat{X}, \hat{\rho} \}$ denotes the standard dissipative superoperator, constructed from an arbitrary linear operator \hat{X} acting on the Hilbert space of our system. We note that related two-photon driven many-body bosonic models have been recently studied numerically [12,14,15].

Equation (1) exhibits a generic tension common to many driven-dissipative systems. The drives favor populating the system with pairs of photons, creating squeezing correlations. This is opposed by the losses, the energy detuning Δ (which makes pair addition nonresonant), and most crucially the interaction U (which is like a number-dependent

detuning). This yields the possibility of phase transitions, where a high density could self-consistently make the drives resonant. While there is no conventional hopping, the nonlocal pair drives can create spatial correlations (and are like an “Andreev-reflection” hopping process). Note that our model could be realized in a variety of setups including superconducting circuits and more conventional quantum optical platforms (see the Supplemental Material [38] for a simple circuit implementation of our model). We also note that our solution is even more general than Eq. (1). As shown in the Supplemental Material [38], for a given set of drive amplitudes M_{ij} , there exists a class of standard hopping terms that can be added to \hat{H} without changing the dissipative steady state. We can thus describe, e.g., bipartite lattices with local hopping and pairing terms.

Our goal in this Letter is to understand the dissipative steady state $\hat{\rho}_{ss}$ of our system, which satisfies $\mathcal{L} \hat{\rho}_{ss} = 0$. Surprisingly, for all parameter values and dimensionalities, this can be done exactly and analytically, using the hidden time-reversal symmetry (HTRS) approach introduced in Refs. [23,24]. This method postulates the existence of an antiunitary operator \hat{T} , in terms of which the associated purification of $\hat{\rho}_{ss}$ (which lives in a doubled Hilbert space),

$$\hat{\rho}_{ss} \equiv \text{Tr}_R |\Psi_{\hat{T}}\rangle \langle \Psi_{\hat{T}}|, \quad |\Psi_{\hat{T}}\rangle \equiv \sum_n \sqrt{p_n} |n\rangle_L \hat{T} |n\rangle_R, \quad (3)$$

satisfies a generalized symmetry constraint [23]. Here $|n\rangle$, p_n are the eigenvectors and eigenvalues of $\hat{\rho}_{ss}$, L denotes states in the physical Hilbert space, and R denotes states in the auxiliary Hilbert space, which is another copy of the physical Hilbert space. The ansatz that \hat{T} is a HTRS implies a set of conditions on $|\Psi_{\hat{T}}\rangle$ that must be solved. For this system, this can be done analytically [38].

The resulting solution for the pure state $|\Psi_{\hat{T}}\rangle$ has a striking form. It describes an unusual kind of pair condensate: all particles occupy the same two-body wave function whose spatial structure is determined by the driving amplitudes M_{ij} . We find [38]

$$|\Psi_{\hat{T}}\rangle = \sum_{m=0}^{\infty} \frac{c_m}{m!} (\hat{K}_+)^m |\Omega\rangle, \quad \hat{K}_+ := \frac{N}{2U} \sum_{ij} M_{ij} \hat{\alpha}_i^\dagger \hat{\alpha}_j^\dagger, \quad (4)$$

where \hat{K}_+ is the effective pair creation operator, $\hat{\alpha}_j \equiv (\hat{a}_{j,L} + \hat{a}_{j,R})/\sqrt{2}$, and $|\Omega\rangle \equiv |0\rangle_L |0\rangle_R$ is the vacuum. The coefficients c_m in the expansion take the simple form

$$c_m \propto (-1)^m / (\delta)_m, \quad (5)$$

where $(\delta)_m := \delta(\delta+1)\cdots(\delta+m-1)$ denotes the Pochhammer symbol (rising factorial), and where the dimensionless detuning parameter r is

$$\delta := 1 - N\Delta_{\text{eff}}/2U, \quad \Delta_{\text{eff}} := \Delta + i\kappa/2. \quad (6)$$

We stress that when $U \neq 0$, this pure-state pair condensate is highly non-Gaussian and exhibits Wigner-function negativity. The parameter dependence of this state is also remarkable. The global Hubbard interaction U along with the detuning Δ and loss κ determine the effective “fugacity” of our pair gas via the c_m coefficients. In contrast, all spatial structure (encoded in M_{ij}) is encoded completely in the two-body “wave function” of each paired boson. Finally, the resulting dissipative steady state is nonthermal, in that it cannot be written as $\exp(-\beta\hat{H})$ for some β [38].

Emergence of phase transitions.—The exact solution allows us to study the emergence of dissipative phase transitions as the number of sites N becomes large, i.e., in the thermodynamic limit. This can be done for arbitrary dimensionality D , and while still remaining in low-density regimes where semiclassical approximations would fail. We find a direct connection between first-order phase transitions that occur at large N , and discrete multiphoton resonances that can be resolved at smaller N . This is seen clearly in Fig. 2(a), which shows the average steady-state photon density versus Δ in a $D = 2$ model, for different system sizes. The discrete resonances at modest N occur when the dimensionless detuning r is close to a negative integer. The exact solution tells us that when $\delta = -n + \epsilon$ with $|\epsilon| \ll 1$, the relative “fugacity” between the $n + 1$ and n pair configurations diverges as $\epsilon \rightarrow 0$: $c_{n+1}/c_n = -1/(n + \delta) = O(\epsilon^{-1})$. This divergence (cut off by κ) leads to an enhanced photon number, and thus sharply-defined resonances occurring at detunings $\Delta_n = 2U(n + 1)/N$ [see Fig. 2(a)]. As $N \rightarrow \infty$, the spacing between resonances vanishes, leading to a first-order phase transition where the density exhibits a jump as a function of Δ . Figure 2(a) also shows a comparison against the predictions of a simple semiclassical mean-field theory (see the Supplemental Material [38] for more details, as well as comparisons to Gutzwiller mean-field theory).

A further virtue of the exact solution is that it gives full access to spatial correlations. We find that these correlations provide a much better way of distinguishing phases compared with purely local observables. In the large- N limit, two-point equal-time correlators in the steady state such as $\langle \hat{a}_{i+r} \hat{a}_i \rangle_{ss}$, $\langle \hat{a}_{i+r}^\dagger \hat{a}_i \rangle_{ss}$ always decay exponentially with distance [see Fig. 2(b)]. In stark contrast, the global Hubbard interaction generates long-range (but weak) density-density correlations. To study this quantitatively, we define in $D = 1$ the reduced density-density correlator

$$g^{(2)}(i, r) := \frac{\langle \hat{n}_{i+r} \hat{n}_i \rangle_{ss} - \bar{n}^2}{\bar{n}^2}. \quad (7)$$

Here, $\bar{n} \equiv \langle \hat{n}_j \rangle_{ss}$ is the mean on site occupation in the steady state, and we note that $g^{(2)}(i, r)$ is independent of i

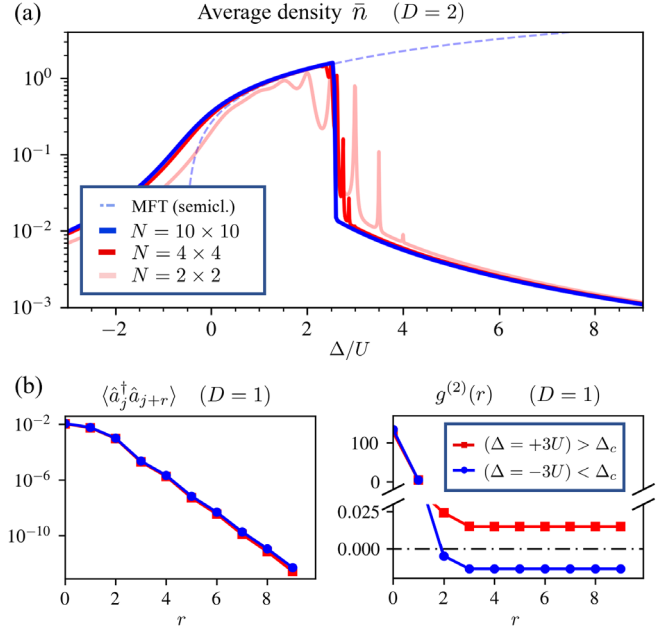


FIG. 2. Driven-dissipative phase transitions. (a) Average density \bar{n} versus detuning Δ for various sized 2D square lattices (periodic boundary conditions, $\kappa = 0.01U$, $G = U/5$, $\Lambda = U/4$). As system size increases, discrete resonances merge to yield a jump in the density and a first-order phase transition. We also show the predictions of a basic semiclassical mean-field theory, which predicts a zero-density solution that cannot be shown here due to the log scale on the y axis. (b) Here, we attempt to distinguish the bunched (red squares) and antibunched (blue circles) phases via their correlations, respectively, single-particle (left panel) and density-density (right panel) correlations. We choose $\Delta = +3U$ as representative of the bunched phase and $\Delta = -3U$ as representative of the antibunched phase. Both plots show data for a $N = 100$ site periodic lattice with $D = 1$. All other parameters are the same as in panel (a). All results are computed using the exact solution in Eq. (4).

away from boundaries. An analogous definition holds for $D > 1$.

We find that the two phases of our model can be cleanly distinguished by the sign of their large-distance density-density correlations, i.e., by $g_\infty^{(2)} \equiv \lim_{|r| \rightarrow \infty} g^{(2)}(r)$. We call the phase where $g_\infty^{(2)} > 0$ a “bunched” phase, where density fluctuations are positively correlated at long distances, and the remaining phase with $g_\infty^{(2)} < 0$ an “antibunched” phase. When κ is sufficiently small, these phases are connected by the first-order phase transition mentioned above. The corresponding jump in density is accompanied by a sign change in $g_\infty^{(2)}$; see Fig. 2(b), right panel. We also note that for modest values of N , the multiphoton resonance physics described above can also lead to interesting structures resembling Mott lobes [9,51], if one looks at intersite correlations. This is shown in Fig. 1(b).

Criticality in the $D = 0$ model.—The above physics becomes especially clear in the limit where $\Lambda \equiv 0$, i.e.,

purely local driving. There is no remaining spatial structure; hence, we call this the $D = 0$ limit. As we saw in Fig. 2, for $D > 0$, our model has a finite correlation length characterizing the decay of two-point correlators. The $D = 0$ model sets this length to zero, while retaining the more interesting physics associated with density-density correlations. The $D = 0$ limit is also experimentally relevant: it can be realized directly using a relatively simple superconducting circuit [38].

The $D = 0$ case has another key virtue: it allows a dramatic simplification in the calculation of observables, as now \hat{K}_+ , \hat{K}_+^\dagger , and $\hat{K}_z \equiv (2NG^2/U)[\hat{K}_+^\dagger, \hat{K}_+]$ form a representation of the Lie algebra of $SU(1,1)$. This makes the problem of evaluating moments with respect to the state $|\Psi_{\hat{\gamma}}\rangle$ given in Eq. (4) completely algebraic; one only requires knowledge of the bosonic representation theory of $SU(1,1)$. Further, harmonic analysis in \mathbb{R}^N yields a satisfactory characterization of the requisite representation theory [38]. We are thus able to compute local observables and correlators for systems with tens of thousands of sites and at unit density. For our $D = 0$ model and for large N , we can verify by brute force that $\lim_{\Delta \rightarrow \Delta_c^\pm} \text{sign}\{g_\infty^{(2)}\} = \pm 1$, where Δ_c denotes the location of the discontinuity in \bar{n} . This confirms that the first-order phase transition (PT) marks the boundary between bunched- and antibunched phases (cf. Fig. 2). We also find that this first-order PT only exists when $\kappa < \kappa_c$, where κ_c is a critical damping threshold, akin to a critical pressure in a liquid-gas transition [cf. Fig. 3(a)]. As in a liquid-gas transition, above the critical point the two phases are smoothly connected, as is indicated by the continuity of $g_\infty^{(2)}$ in Fig. 3(b). Here, we use the exact solution to estimate κ_c , by explicitly observing the

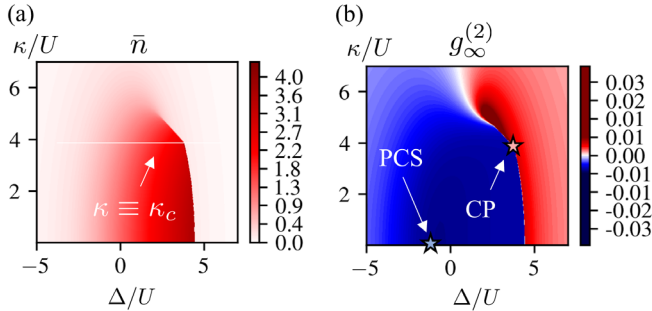


FIG. 3. Phase diagram for $D = 0$. (a) Average density as a function of detuning Δ and loss κ , with $N = 500$, $\Lambda = 0$, and $G = U$. Phase boundaries can be seen, and the critical damping value κ_c is also indicated: for $\kappa > \kappa_c$, the first-order PT vanishes. (b) Asymptotic long-distance behavior of the density-density correlation function, as captured by $g_\infty^{(2)}$ [cf. Eq. (7)]; the sign of this quantity more clearly distinguishes the two relevant phases in the model. A critical point $\Delta_{\text{eff}}^c := \Delta_c + i\kappa_c/2$ marks the exact location where $g_\infty^{(2)}$ becomes continuous across the phase boundary. Same parameters as in panel (a). The parameter tuning that results in a many-body pair-coherent state is indicated with a star.

divergence of the susceptibility $\chi \equiv \partial \bar{n} / \partial \Delta$ as $\kappa \rightarrow \kappa_c^+$; see the Supplemental Material [38] for more details.

Many-body pair-coherent states.—When $D > 0$, analysis based on the exact solution becomes more challenging. One can still obtain a representation of the Lie algebra $SU(1,1)$ by defining a (generalized) pair-lowering operator $\hat{K}_- := (U/2N) \sum_{ij} (M^{-1})_{ij} \hat{\alpha}_i \hat{\alpha}_j$, which has the effect of removing a pair of bosons: $\hat{K}_- \hat{K}_+^m |\Omega\rangle \propto \hat{K}_+^{m-1} |\Omega\rangle$. However, \hat{K}_- is not equal or proportional to \hat{K}_+^\dagger unless $D \equiv 0$ or $D \equiv \infty$. The result is that representation-theoretic techniques are of no utility when $D > 0$. Nonetheless, the Lie-theoretic point of view is still useful in helping reveal unusual phenomena.

In particular, at special detuning values, the gas of boson pairs constituting the purification of the steady state [cf. Eq. (4)] forms a many-body pair-coherent state (PCS), that is, an eigenstate of the operator \hat{K}_- [33]. From the form of the solution, we see that this happens when $c_{m+1}/c_m = -k/(N/2 + m)$, where $k = -1$ is the corresponding eigenvalue of \hat{K}_- [38]. From Eq. (6), we see that this requires $\delta = N/2$, corresponding to $\kappa \rightarrow 0^+$ and

$$\Delta \rightarrow \Delta_{\text{PCS}} := U(2 - N)/N. \quad (8)$$

Note that for the case of just a single mode $N = 1$, this corresponds to the known physics of a Kerr parametric oscillator [26]. In this case, $\Delta = U$ is the same as zero detuning if one normal orders the Kerr interaction, and $|\Psi_{\hat{\gamma}}\rangle$ reduces to an even-parity cat state.

We stress that there are observable consequences associated with the formation of this many-body PCS. As one approaches the special detuning, there are no fluctuations in the global pairing, as quantified by the operator \hat{K}_- . One can explicitly show that

$$\left\langle \left(\sum_{ij} (M^{-1})_{ij} \hat{a}_i \hat{a}_j \right)^{\dagger n} \left(\sum_{ij} (M^{-1})_{ij} \hat{a}_i \hat{a}_j \right)^m \right\rangle_{\text{ss}, \Delta \rightarrow \Delta_{\text{PCS}}} \propto k^{*n} k^m. \quad (9)$$

Similar to their two-mode counterparts [52,53], the many-body PCS we describe here may have utility for bosonic quantum error correction [36,37,54–56]. We note that the many-body PCS that emerge here are distinct from the multimode states discussed in Ref. [35].

Symmetry breaking.—In the strong-driving regime, our model exhibits a surprising symmetry breaking phenomenon. First, note that the singular values of our matrix of pair-driving amplitudes is $\lambda_{\mathbf{k}} = (1/u)|(\Lambda/D) \sum_{j=1}^D \cos k_j + G|$ where the wave vector \mathbf{k} labels standing wave modes. Let λ_* denote the maximum singular value, and s denote the number of distinct modes that it corresponds to (so-called max pairing modes). For large driving, one can analytically show that the steady-state Wigner function $W[\{\alpha_{\mathbf{k}}\}]$ corresponds to a uniform distribution over the $(s - 1)$ -sphere defined by

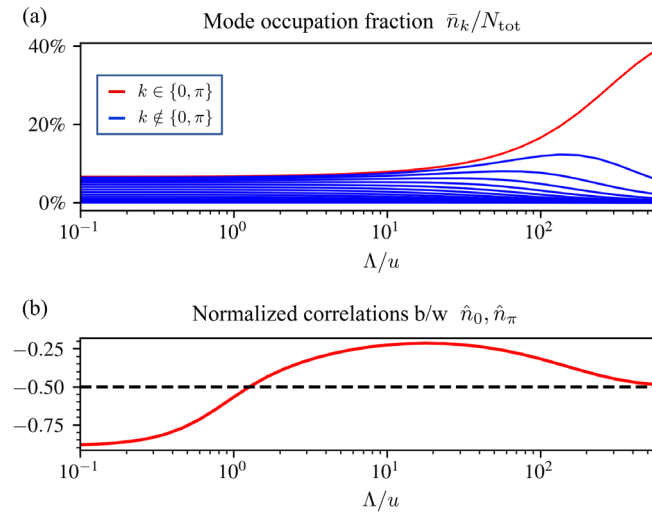


FIG. 4. Symmetry breaking at strong driving. (a) Occupancy \bar{n}_k of standing wave modes in an odd-length $D = 1$ open chain, as the drive Λ is increased. For large drives, the modes with the largest pairing amplitudes, $k = 0, \pi$, dominate. N_{tot} denotes average total photon number. Parameters are $\Delta = 0$, $\kappa = u/100$, $u \equiv U/N$, $N = 31$. (b) Normalized density correlations between the modes at $k = 0, \pi$ (red curve), and the horizontal asymptote $y \equiv -1/s$ predicted by a uniform sphere distribution (black dashed line). Here, $s = 2$. Parameters same as in panel (a).

$$\sum_{\lambda_{\mathbf{k}}=\lambda_s} x_{\mathbf{k}}^2 = \text{const}, \quad x_{\mathbf{k}} \equiv e^{-i\theta} \alpha_{\mathbf{k}} \quad (10)$$

with $x_{\mathbf{k}} \in \mathbb{R}$ and θ an overall phase [38]. Even though there is a near continuum of pairing eigenvalues, for large driving, the max pairing modes completely dominate. This behavior is shown explicitly in Fig. 4(a). The structure of this solution also directly leads to an anticorrelation between mode amplitudes that is purely geometric; see Fig. 4(b).

The mode selection in our system can be related to spontaneous symmetry breaking. Real rotations amongst the max-pairing modes form a non-Abelian group of weak symmetries isomorphic to $O(s, \mathbb{R})$ which commutes with the Lindbladian \mathcal{L} . At high driving strengths we conjecture that this symmetry is spontaneously broken. This is seen clearly at the semiclassical level, where one can show [38] that every point on the max pairing $(s - 1)$ -sphere is a *stable* stationary state of the dynamics. Each such solution of course breaks the underlying mode-rotation symmetry. In the full quantum theory, fluctuations lead to a slow randomization on this space of symmetry broken solutions, yielding the final unique steady state. The effective mode selection phenomena in our model is reminiscent (but not identical to) of analogous effects in other systems (see, e.g., Refs. [57–59]). Reference [60] also describes (using semiclassical mean field theory) related phenomena in a many-mode model with uniform pairing, with mode selection being controlled by dispersion as opposed to pairing

amplitudes. We stress that in contrast to Ref. [60] our exact solution lets us describe all quantum fluctuation effects, allowing analytical insights into how our mode selection effect emerges as the dimensionless driving rates G/U , Λ/U become large; see Fig. 4(a).

Discussion.—We have introduced a class of strongly interacting, two-photon driven bosonic lattice models whose dissipative steady states can be found exactly. The models exhibit a wealth of interesting phenomena, including emergent phase transitions, many-body pair coherent states, and novel mode competition and symmetry breaking. Our work provides an important means for benchmarking approximation techniques, and also reveals that the physics of Kerr parametric oscillators (studied extensively for error correction) is even richer in the many-body limit. It also suggests that the HTRS solution method could be used to successfully address a host of truly many-body problems.

We thank Alexander McDonald, Qian Xu, and Mark Dykman for helpful discussions. This work was supported by the Air Force Office of Scientific Research MURI program under Grant No. FA9550-19-1-0399, and the Simons Foundation through a Simons Investigator award (Grant No. 669487).

*Corresponding author.

droberts01@uchicago.edu

- [1] K. Baumann, C. Guerlin, F. Brennecke, and T. Esslinger, *Nature (London)* **464**, 1301 (2010).
- [2] A. A. Houck, H. E. Türeci, and J. Koch, *Nat. Phys.* **8**, 292 (2012).
- [3] M. Fitzpatrick, N. M. Sundaresan, A. C. Y. Li, J. Koch, and A. A. Houck, *Phys. Rev. X* **7**, 011016 (2017).
- [4] T. Fink, A. Schade, S. Höfling, C. Schneider, and A. Imamoglu, *Nat. Phys.* **14**, 365 (2018).
- [5] R. Ma, B. Saxberg, C. Owens, N. Leung, Y. Lu, J. Simon, and D. I. Schuster, *Nature (London)* **566**, 51 (2019).
- [6] S. Diehl, A. Micheli, A. Kantian, B. Kraus, H. P. Büchler, and P. Zoller, *Nat. Phys.* **4**, 878 (2008).
- [7] Emanuele G. Dalla Torre, S. Diehl, M. D. Lukin, S. Sachdev, and P. Strack, *Phys. Rev. A* **87**, 023831 (2013).
- [8] L. M. Sieberer, S. D. Huber, E. Altman, and S. Diehl, *Phys. Rev. Lett.* **110**, 195301 (2013).
- [9] A. LeBoite, G. Orso, and C. Ciuti, *Phys. Rev. Lett.* **110**, 233601 (2013).
- [10] M. J. Hartmann, *J. Opt.* **18**, 104005 (2016).
- [11] A. Biella, F. Storme, J. Lebreuilly, D. Rossini, R. Fazio, I. Carusotto, and C. Ciuti, *Phys. Rev. A* **96**, 023839 (2017).
- [12] V. Savona, *Phys. Rev. A* **96**, 033826 (2017).
- [13] M. I. Dykman, C. Bruder, N. Lörch, and Y. Zhang, *Phys. Rev. B* **98**, 195444 (2018).
- [14] J. Lebreuilly, C. Aron, and C. Mora, *Phys. Rev. Lett.* **122**, 120402 (2019).
- [15] R. Rota, F. Minganti, C. Ciuti, and V. Savona, *Phys. Rev. Lett.* **122**, 110405 (2019).

- [16] D. S. Rokhsar and B. G. Kotliar, *Phys. Rev. B* **44**, 10328 (1991).
- [17] W. Krauth, M. Caffarel, and J.-P. Bouchaud, *Phys. Rev. B* **45**, 3137 (1992).
- [18] W. Krauth, M. Caffarel, and J.-P. Bouchaud, *Phys. Rev. B* **45**, 3137 (1992).
- [19] W. Zwerger, *J. Opt. B* **5**, S9 (2003).
- [20] E. Mascarenhas, H. Flayac, and V. Savona, *Phys. Rev. A* **92**, 022116 (2015).
- [21] S. Finazzi, A. LeBoite, F. Storme, A. Baksic, and C. Ciuti, *Phys. Rev. Lett.* **115**, 080604 (2015).
- [22] O. Scarlatella, A. A. Clerk, R. Fazio, and M. Schiró, *Phys. Rev. X* **11**, 031018 (2021).
- [23] D. Roberts, A. Lingenfelter, and A. A. Clerk, *PRX Quantum* **2**, 020336 (2021).
- [24] K. Stannigel, P. Rabl, and P. Zoller, *New J. Phys.* **14**, 063014 (2012).
- [25] P. D. Drummond and D. F. Walls, *J. Phys. A* **13**, 725 (1980).
- [26] M. Wolinsky and H. J. Carmichael, *Phys. Rev. Lett.* **60**, 1836 (1988).
- [27] G. Y. Kryuchkyan and K. V. Kheruntsyan, *Opt. Commun.* **127**, 230 (1996).
- [28] K. V. Kheruntsyan, D. S. Krähmer, G. Y. Kryuchkyan, and K. G. Petrossian, *Opt. Commun.* **139**, 157 (1997).
- [29] G. Kryuchkyan, K. Kheruntsyan, V. Papanyan, and K. Petrossian, *Quantum Semiclassical Opt.* **7**, 965 (1999).
- [30] B. Cao, K. W. Mahmud, and M. Hafezi, *Phys. Rev. A* **94**, 063805 (2016).
- [31] K. V. Kheruntsyan and K. G. Petrosyan, *Phys. Rev. A* **62**, 015801 (2000).
- [32] F. Minganti, N. Bartolo, J. Lolli, W. Casteels, and C. Ciuti, *Sci. Rep.* **6**, 26987 (2016).
- [33] A. O. Barut and L. Girardello, *Commun. Math. Phys.* **21**, 41 (1971).
- [34] S. Luo, *J. Math. Phys. (N.Y.)* **38**, 3478 (1997).
- [35] V. V. Albert, S. O. Mundhada, A. Grimm, S. Touzard, M. H. Devoret, and L. Jiang, *Quantum Sci. Technol.* **4**, 035007 (2019).
- [36] A. Grimm, N. E. Frattini, S. Puri, S. O. Mundhada, S. Touzard, M. Mirrahimi, S. M. Girvin, S. Shankar, and M. H. Devoret, *Nature (London)* **584**, 205 (2020).
- [37] R. Lescanne, M. Villiers, T. Peronnin, A. Sarlette, M. Delbecq, B. Huard, T. Kontos, M. Mirrahimi, and Z. Leghtas, *Nat. Phys.* **16**, 509 (2020).
- [38] See Supplemental Material at <http://link.aps.org/supplemental/10.1103/PhysRevLett.130.063601> for more theoretical details, as well as an experimental scheme that realizes our model using a superconducting circuit. The SM includes Refs. [39–50].
- [39] J. E. Moyal, *Math. Proc. Cambridge Philos. Soc.* **45**, 99 (1949).
- [40] P. Wang and R. Fazio, *Phys. Rev. A* **103**, 013306 (2021).
- [41] S. Axler, P. Bourdon, and W. Ramey, *Harmonic Function Theory*, 2nd ed., Graduate Texts in Mathematics Vol. 137 (Springer, New York, 2001).
- [42] S. Axler, HFT.m version 12.03 (2020), https://www.axler.net/HFT_Math.html.
- [43] D. Roberts and A. A. Clerk, *Phys. Rev. X* **10**, 021022 (2020).
- [44] V. Bargmann, *Commun. Pure Appl. Math.* **14**, 187 (1961).
- [45] V. Bargmann, *Commun. Pure Appl. Math.* **20**, 1 (1967).
- [46] O. Scarlatella, A. A. Clerk, R. Fazio, and M. Schiró, *Phys. Rev. X* **11**, 031018 (2021).
- [47] L. Autonne, *Sur les Matrices Hypohermitiennes et sur les Matrices Unitaires* (A. Rey, Lyon, 1915).
- [48] F. Fagnola and V. Umanità, *Commun. Math. Phys.* **298**, 523 (2010).
- [49] H. U. Strand, M. Eckstein, and P. Werner, *Phys. Rev. X* **5**, 011038 (2015).
- [50] B. Buča and T. Prosen, *New J. Phys.* **14**, 073007 (2012).
- [51] A. LeBoite, G. Orso, and C. Ciuti, *Phys. Rev. A* **90**, 063821 (2014).
- [52] G. S. Agarwal, *J. Opt. Soc. Am. B* **5**, 1940 (1988).
- [53] G. S. Agarwal and A. Biswas, *J. Opt. B* **7**, 350 (2005).
- [54] M. Mirrahimi, Z. Leghtas, V. V. Albert, S. Touzard, R. J. Schoelkopf, L. Jiang, and M. H. Devoret, *New J. Phys.* **16**, 045014 (2014).
- [55] Z. Leghtas, S. Touzard, I. M. Pop, A. Kou, B. Vlastakis, A. Petrenko, K. M. Sliwa, A. Narla, S. Shankar, M. J. Hatridge, M. Reagor, L. Frunzio, R. J. Schoelkopf, M. Mirrahimi, and M. H. Devoret, *Science* **347**, 853 (2015).
- [56] S. Puri, A. Grimm, P. Campagne-Ibarcq, A. Eickbusch, K. Noh, G. Roberts, L. Jiang, M. Mirrahimi, M. H. Devoret, and S. M. Girvin, *Phys. Rev. X* **9**, 041009 (2019).
- [57] L. M. Narducci, J. R. Tredicce, L. A. Lugiato, N. B. Abraham, and D. K. Bandy, *Phys. Rev. A* **33**, 1842 (1986).
- [58] M. Gong, Y. Yuan, C. Li, P. Yan, H. Zhang, and S. Liao, *Opt. Express* **15**, 3236 (2007).
- [59] J. R. Stone, G. Moille, X. Lu, and K. Srinivasan, *Phys. Rev. Appl.* **17**, 024038 (2022).
- [60] Z. Wang, C. Navarrete-Benlloch, and Z. Cai, *Phys. Rev. Lett.* **125**, 115301 (2020).